Polymer Journal (2018) 50:951–958
https://doi.org/10.1038/s41428-018-0083-1

FOCUS REVIEW

Soft materials based on colloidal self-assembly in ionic liquids

Kazuhide Ueno[1]

Received: 23 February 2018 / Revised: 25 April 2018 / Accepted: 26 April 2018 / Published online: 6 June 2018

Abstract

Ionic liquids (ILs) have attracted much attention as dispersion media for colloidal systems as alternatives to organic solvents and electrolyte solutions. Although colloidal stability is an essential factor for determining the properties and performance of colloidal systems containing ILs, detailed mechanisms for colloidal stabilization have not yet been studied. In the first part of this paper, we highlight our fundamental studies on colloidal stability. Three different repulsive forces, electrostatic, solvation, and steric interactions, are examined for their effectiveness in stabilizing colloidal particles in ILs. In the second part of this report, we provide an overview of our recent studies on colloidal soft materials in the presence of ILs. On the basis of the suspended state of the silica colloid particles, two different soft materials, a colloidal gel and a colloidal glass, were prepared in ILs. Their functional properties, including ionic transport, rheological, and optical properties, are discussed in relation to the microstructures of the colloidal materials.

Introduction

Gel materials containing an ionic liquid (IL) have received much attention for a variety of applications because they can be handled as solid materials with inherent, IL-derived, unique properties that are not found in molecular liquids [1, 2]. For instance, high thermal stability, high ionic conductivity, and a wide electrochemical potential window have been exploited in an IL-based solid-state electrolyte for electrochemical devices (e.g., solid-state secondary batteries, fuel cells, solar cells, field-effect transistors, and ionic polymer actuators) [3, 4]. The highly selective solubility of certain compounds (especially CO_2) and very low vapor pressure are considered attractive characteristics of ILs for membrane separation technology; there have been several reports of IL-based separation membranes in this area of research [5–7].

Solid-like mechanical properties can generally be introduced into ILs by forming organic or inorganic three-dimensional networks in the ILs. Polymer gels containing ILs can be prepared by the in situ polymerization of monomers and cross-linkers [8] or by the self-assembly of ABA tri-block copolymers [9] if the A and B segments are insoluble and soluble in the ILs, respectively. Certain polymers that undergo micro-phase separation can also be converted into self-supporting polymeric membranes in the presence of ILs [10–12]. Inorganic networks have been constructed by in situ sol–gel reactions of metal alkoxides in ILs, in which the porous skeletons of the resulting metal oxide monoliths (e.g., silica) are impregnated with the ILs [13]. Another facile procedure for obtaining gel-like materials from ILs is to employ the colloidal assembly of nanoparticles (NPs) in ILs [14], and we highlight recent studies on this class of soft materials in this paper.

The fluidity of a colloidal suspension may be entirely lost when the particle concentration increases to a certain critical concentration (known as the jamming transition) [15]. There are two categories of solid-like soft materials consisting of colloidal suspensions, colloidal gels and colloidal glasses, based on the internal structure of the particle assembly (Fig. 1) [16]. A colloidal gel is generally formed with colloidally unstable particles in a medium where the interparticle attractive forces are dominant. The particles aggregate into a fractal-like network, which percolates through the bulk of the suspension even at relatively small particle concentrations. On the other hand, colloidal glass is often formed with colloidally stable, repulsive particles. In suspensions with concentrations above the critical particle

✉ Kazuhide Ueno
ueno-kazuhide-rc@ynu.ac.jp

[1] Department of Chemistry and Biotechnology, Yokohama National University, 79-5 Tokiwadai, Hodogaya-ku, Yokohama 240-8501, Japan

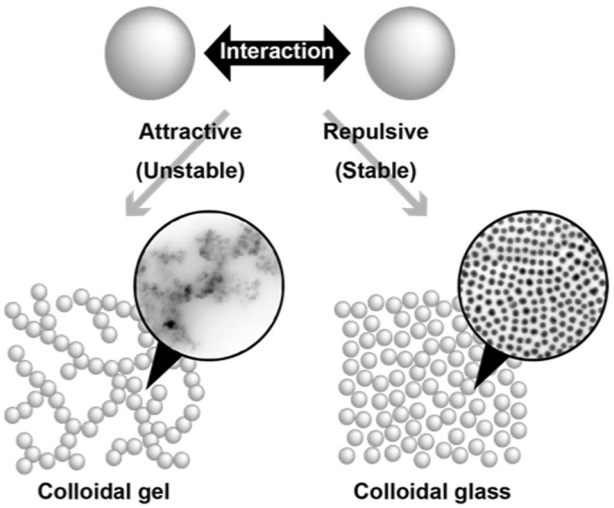

Fig. 1 Schematic illustration of the colloidal gel and colloidal glass formed with unstable and stable nanoparticles (NPs), respectively. Representative TEM images of the soft colloidal materials formed in the ILs: (left) 5 wt% fumed silica NPs ($R = 6$ nm) in [C_2mim][NTf_2] and (right) 16.7 wt% poly(methyl methacrylate) (PMMA)-grafted silica NPs ($M_n = 53$ kDa) in [C_2mim][NTf_2]

concentration, the translational motion of each particle is inhibited by the crowding of neighboring particles (cage effect) [17]. Therefore, the entire system gets trapped into a metastable frozen state and shows a solid-like response.

Although the formation of soft materials is governed primarily by the colloidal interactions as mentioned above, the details of the interparticle attractive and repulsive forces in ILs is not yet understood. In connection with the applications of colloidal systems containing ILs, there have been several works on the synthesis of metal and semiconductor NPs [18], on the catalytic processes using noble metal NPs [19], and on the preparation of functional NP-IL composites; [20, 21] some of these works have reported unusual enhancements in the colloidal stability of the NPs in ILs in the absence of additional stabilizers. Hence, understanding the colloidal stability of NPs in ILs is also an important research topic. In this respect, our group has been investigating silica NPs as a model while keeping the following queries in mind: (1) how the NPs are stabilized in the ILs? (2) What type of repulsions is actually effective in stabilizing the NPs in the ILs? and (3) can we prepare the above two colloid-based soft materials in the presence of ILs? In the first part of this paper, we report our fundamental studies on the interparticle interactions acting in ILs. In the second part, we discuss the functional properties of the colloidal gels and colloidal glasses containing ILs.

Interparticle forces in ILs

The colloidal stability of NPs in suspensions is determined by the combination of attractive/repulsive forces; the NPs can be kinetically stabilized when the repulsive forces are much stronger than the attractive forces. Van der Waals forces are universal and are the predominant attractive force in the colloidal system [22]. Unlike the molecules in molecular systems, colloidal NPs are considered molecular assemblies of a large number of molecules; for this reason, van der Waals potential energy (V_{vdw}) generates strong and long-range attractions that are proportional to the radius of the NPs (R) and inversely proportional to the interparticle distance (D). This is strong enough to form the colloidal aggregates if no effective repulsions are present. In addition, V_{vdw} is a function of refractive index of not only the NPs but also the medium, and smaller difference between these two refractive indices leads to weaker V_{vdw} values. The matching of the refractive indices of the silica and the used IL allowed us to minimize the V_{vdw} in the colloidal systems studied here.

Electrostatic forces are a repulsive force derived from the electrical double layer (EDL) of a charged NP [23]. Most importantly, electrostatic potential energy (V_{ele}) strongly depends on the ionic concentration in the medium. The thickness of the EDL decreases as the ionic concentration increases, and V_{ele} is weaker in more concentrated salt solutions. Therefore, it is easy to imagine that V_{ele} would not be effective in an IL in which there is severe charge screening due to an extremely high ionic concentration of the IL.

Considering the van der Waals attractions and electrostatic repulsions, colloidal stability can be simply described on the basis of Derjaguin–Landau–Verwey–Overbeek (DLVO) theory in which $V_{total} = V_{vdw} + V_{ele}$ [23]. Even considering silica-IL systems with a reliable surface charge potential of −38 mV, V_{total} only shows an attractive interaction between the silica particles over various separations (D), as seen in Fig. 2a. Although different ILs with reasonable surface charge potentials ranging from −38 to −52 mV were also examined in the same manner, all the interparticle interaction profiles indicated similar attractive interactions at all the separations. This prediction, made using DLVO theory, can be verified through dynamic light scattering (DLS) experiments, which show aggregates of silica NPs ($R = 60$ nm) suspended in the ILs [24].

To determine the presence or absence of repulsive interactions between silica NPs, the fractal-like aggregation was further investigated on the basis of two different models of cluster–cluster aggregation, diffusion-limited aggregation (DLA), and reaction-limited aggregation (RLA) [25]. Every particle collision causes aggregation in DLA; however, aggregates are only formed when the particle collision overcomes a moderate energy barrier comparable to or larger than kT in RLA. Therefore, the fractal aggregation has a loosely packed structure and a denser structure in DLA and RLA, respectively. The aggregates were formed

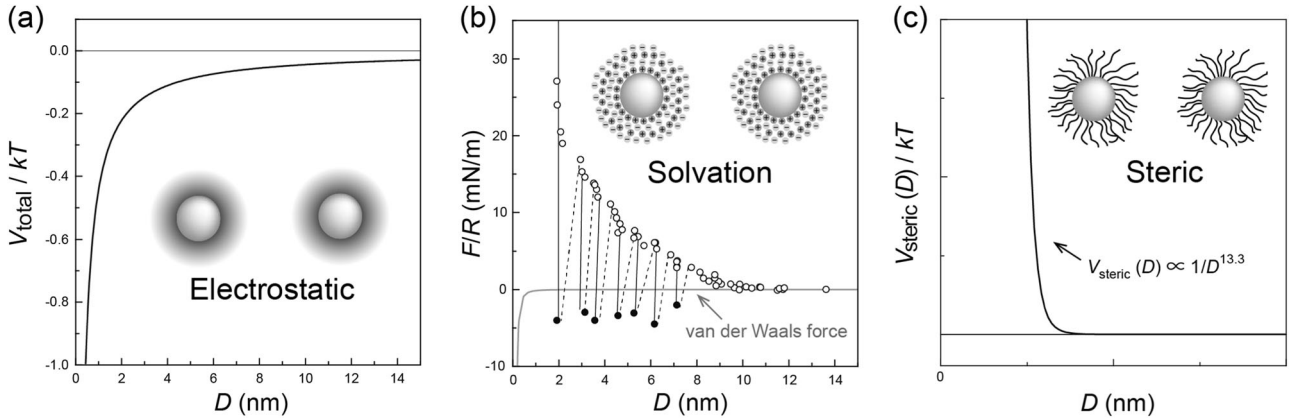

Fig. 2 **a** Total potential energy (V_{total}/kT), calculated for negatively charged silica NPs ($R = 60$ nm) in [C_2mim][NTf_2]. **b** Normal force scaled with the surface radius of curvature (F/R) as a function of the surface separation (D) between silica surfaces in [C_4mim][NTf_2]; the gray solid line represents the calculated van der Waals force. **c** Predicted steric repulsive force between the PMMA-grafted silica NPs ($M_n = 132$ kDa) in [C_2mim][NTf_2]

through RLA in an IL, [C_2mim][NTf_2] [26], while DLA was reported for the same silica NPs suspended in mineral oil [27]. This implies that another repulsive force is present between the silica NPs; the non-electrostatic repulsions, however, were not strong enough to stabilize the silica NPs in the case of [C_2mim][NTf_2]. It was found that the same silica NPs are well stabilized in BF_4-based ILs by the non-electrostatic repulsions [28].

Figure 2b shows actual surface force (F/R) between the silica surfaces in an IL, which was measured using a surface force apparatus [29]. The surface force measurement revealed the presence of a non-electrostatic repulsive force. When liquid molecules are confined to the nanoscale, the repulsion has an oscillatory profile that can be attributed to the solvation force resulting from the formation of a layered structure in the vicinity of solid surfaces [30]. Similar layer-by-layer structures of cations and anions of the ILs on charged surfaces have also been suggested by AFM measurements, high-energy X-ray reflectivity measurements, and molecular dynamics simulations [31]. The intrinsic structure-forming properties of bulk ILs would lead to the formation of remarkably well-defined layered structures at charged surfaces. Although many ILs were found to show solvation forces [32] and this can be an efficient repulsion for stabilizing NPs in the highly ionic media, the colloidal stabilization of NPs by the IL-based solvation force was found in few cases. In addition to the above-mentioned BF_4-based ILs, the unusual stabilization by the IL-based solvation forces was reported for silica NPs suspended in a protic IL, ethyl ammonium nitrate [33]. A recent study showed that surface-ion hydrogen bonding leads to a strong solvation force and enabling the colloidal stabilization in this type of ILs [34]. It was also recently reported that metal and semiconductor NPs can be stabilized by a layer of surface-bound ions in inorganic ILs [35].

The steric repulsion, derived from the excluded volume effect of surface functional groups on the NPs, was examined using poly(methyl methacrylate)-grafted silica NPs (PMMA-*g*-NPs) in ILs. In a good solvent, the penetration of the grafted polymers gives rise to a repulsion between the polymer-grafted NPs [36]. The observations by DLS and TEM proved that PMMA-*g*-NPs, where PMMA is soluble, are suspended as primary particles without aggregation in the ILs [24]. Rheological measurements of the concentrated suspensions of PMMA-*g*-NPs, having $M_n = 132$ kDa, have also shown that PMMA-*g*-NPs have a soft repulsive potential energy ($V_{steric}(D)$) proportional to $D^{-13.3}$ in [C_2mim][NTf_2] [37], which is due to the deformable outer shell of the grafted PMMA molecules swollen with [C_2mim][NTf_2] (Fig. 2c).

The colloidal stability of PMMA-*g*-NPs was also studied in various ILs since the steric interaction is dominated by the solubility of the grafted polymer in the medium [38]. V_{steric} (D) is attractive in a poor solvent for the grafted polymer. In other words, the DLS measurements of PMMA-*g*-NPs enabled us to evaluate the solubility of the PMMA in the ILs. Figure 3 shows the hydrodynamic radii (R_h values) of the PMMA-*g*-NPs in the alkylimidazolium ILs with different alkyl chain lengths and anionic structures. The PMMA-*g*-NPs were aggregated in all the BF_4-based ILs, defined as $R_h = 60$ nm in Fig. 3, because of the insolubility of the PMMA in these ILs. The R_h became larger in the ILs with more hydrophobic anions in the following order: [TfO] < PF_6 < [NTf_2]-based ILs. When the anionic structure is the same, R_h is closely related to the nonpolar solubility parameter (δ_{NP}), which was proposed by Coutinho et al. [39], and reaches its maximum at $\delta_{NP} =$ ~22 $MPa^{0.5}$. The above study suggests that the whole balance between the nonpolar characteristics of the cations and anions is associated with the solubility of the PMMA. The effect of the nonpolarity of the anion has a greater

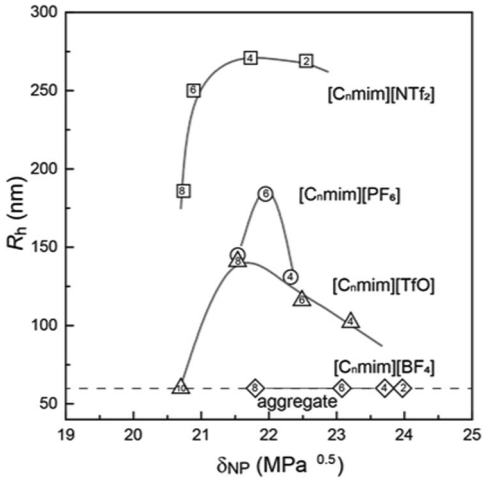

Fig. 3 Hydrodynamic radii (R_h values) of PMMA-*g*-NPs ($M_n = 180$ kDa) in [$C_n$mim]-based ILs with various anionic structures at 25 °C plotted as a function of the nonpolar solubility parameter (δ_{NP}) of the ILs (reported by Coutinho et al.) [39]

impact on the solubility; the nonpolarity of the cation also modifies the overall affinity toward PMMA.

Through the fundamental studies on the interparticle interactions in ILs, the following answers were found for the original questions about the colloidal stability of NPs in ILs. The electrostatic repulsion was found to be inefficient due to the concentrated ionic environment in the ILs. Alternatively, the solvation and steric forces have the potential to stabilize the NPs in the ILs. Therefore, IL-based steric and IL-based solvation forces could explain the reported experimental findings of the pronounced colloidal stability in ILs in absence of a stabilizer.

Colloidal gels and colloidal glasses in ILs

IL-based colloidal gels can be readily prepared by mixing, for example, unstable, fumed silica NPs with ILs. The poorly stable silica NPs form interconnected networks with a fractal structure in the ILs, as shown in Fig. 1. Gelation of [C_2mim][NTf_2] could be achieved with the addition of only ≥2 wt% (≥1.5 vol%) of fumed silica NPs with an average radius (R) of 6 nm [26]. The system showed a higher elastic modulus (G') than viscous modulus (G'') in the rheological measurements by dynamic frequency-sweeps, which is characteristic of a soft-solid-like material. On the other hand, a larger particle concentration was required to prepare the IL-based colloidal glass [37]. The particle concentration required for the quasi-solidification was 6 wt% for PMMA-*g*-NPs ($M_n = 132$ kDa). This corresponds to an effective volume fraction (ϕ_{eff}) of ~70–74 vol%, including the silica core and the solvated shell of the PMMA. The ϕ_{eff} value was almost independent of the M_n of the grafted PMMA in PMMA-*g*-NPs, but it was higher than the volume fraction of random close packing for a hard sphere system (~64 vol%) owing to the soft repulsive potential of the PMMA-*g*-NPs (i.e., the deformability of the PMMA shell). The colloidal crystals of PMMA-*g*-NPs in [C_4mim][NTf_2] were prepared by Ohno et al. [40], and the volume fractions of the PMMA-*g*-NPs for freezing and melting were reported to be 23.3 and 24.9 vol%, respectively.

As the loosely bound network could have been disrupted under sufficient shear stress, the colloidal gel showed a reversible "shear thinning" behavior (Fig. 4) [28]. The gel modulus (G') increased with the particle concentration and reached ~10^6 Pa at 15 wt%. The ionic structures of ILs were found to affect the formation of colloidal gels. Indeed, no gelation occurred with the same fumed silica NPs in BF_4-based ILs in which the silica NPs were stabilized by the IL-based solvation forces, as discussed in the previous section. These stable suspensions exhibited an interesting "shear thickening" response (Fig. 4) [28]. The sudden increase in shear viscosity can probably be attributed to the temporary aggregation of NPs, which is associated with the collapsing of the surface solvation structure of the ions at an intermediate shear rate. Further dissociation of the aggregates is responsible for the decrease in viscosity at a high shear rate. The colloidal glass of PMMA-*g*-NPs also exhibited shear thinning behavior and a significant increase in the gel modulus with an increase in the particle concentration [37].

One of the important properties of IL-based soft materials is their ionic transport properties. The addition of fumed silica NPs ($R = 6$ nm) had little impact on the ionic conductivity of the colloidal gel with [C_2mim][NTf_2] [26]. The ionic conductivity was lower for the colloidal glasses (Fig. 5a) [37]. The ionic conduction was more inhibited by their interactions with PMMA in addition to the obstruction by the silica NPs. Diffusivity measurements using pulsed field gradient (pfg)-NMR have shown different interactions of the ion-NPs in the colloidal gel and colloidal glass, where D_0 and D_g are the self-diffusion coefficients of the ions in the parent IL and in the soft material, respectively. As seen in Fig. 5b, the higher diffusivity ratio (D_g/D_0) of the cation in the colloidal glass suggests the preferential interaction of $[NTf_2]^-$ anions with PMMA, while the higher D_g/D_0 of the anion in the colloidal gel is indicative of the preferential interaction of the $[C_2mim]^+$ cations with the silica surface. The importance of IL-based colloidal gels has been recognized in the recent studies on all-solid-state lithium-ion batteries in which a colloidal gel was used as a solid electrolyte [41, 42]. The above results provide insight into the role of the interactions of ion-NPs in the development of selective ion-conductive materials and highly ion-conductive materials with high transference numbers of specific ions for energy storage devices.

Temperature sensitivity can be introduced into the grafted polymer for polymer-grafted NPs. In this way, the colloidal stability in the ILs could be thermally controlled.

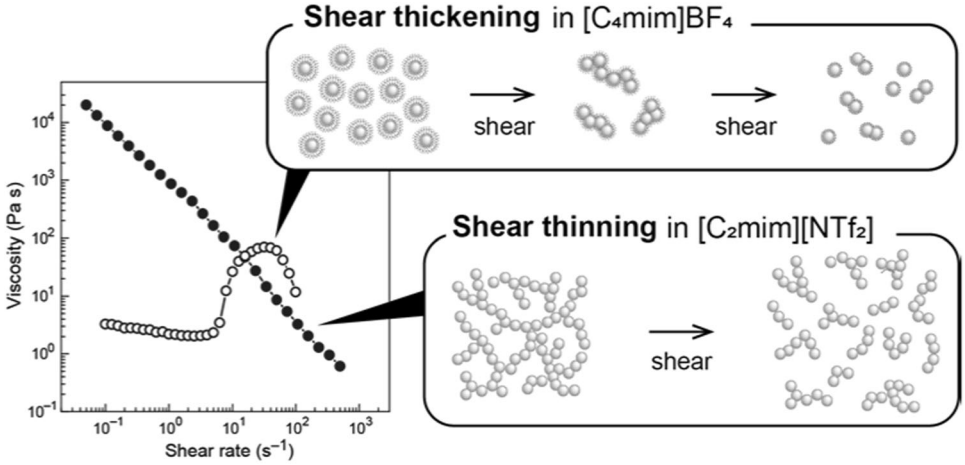

Fig. 4 Shear rate dependence of viscosity for a colloidal gel (closed circle) with 5 wt% fumed silica NPs ($R = 6$ nm) in [C_2mim][NTf_2] and a stable suspension (open circle) with 15 wt% fumed silica NPs in [C_4mim][BF_4], and schematic illustrations of the changes in the microstructures by shear

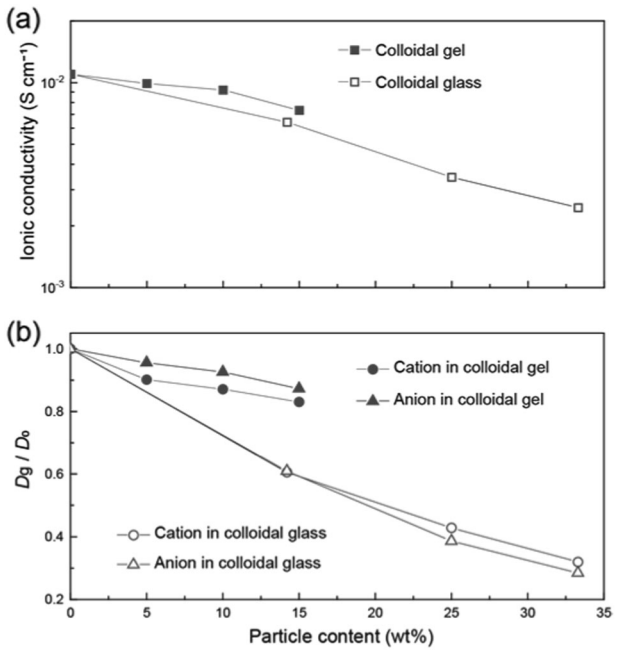

Fig. 5 Dependence of (**a**) ionic conductivity and (**b**) diffusivity ratio (D_g/D_0) on the particle content in the colloidal gel of fumed silica NPs ($R = 6$ nm) in [C_2mim][NTf_2] and for the colloidal glass of PMMA-*g*-NPs ($M_n = 91$ kDa) in [C_2mim][NTf_2] at 30 °C

Poly(benzyl methacrylate) (PBnMA) is known to show a lower critical solution temperature phase separation in certain ILs at the phase separation temperature (T_c) [43]. The PBnMA-*g*-NPs can be sterically stabilized by the solvated PBnMA shell at a low temperature, whereas the PBnMA shell gets desolvated and the PBnMA-*g*-NPs forms aggregates above the T_c. The colloidal glass of PBnMA-*g*-NPs could be formed in [C_2mim][NTf_2] in a similar way as was used for PMMA-*g*-NPs, and it undergoes a transition from colloidal glass to colloidal gel in response to temperature, as seen in TEM images in Fig. 6 [44]. This transition was also characterized as a V-shaped rheological response. Both G' and G'' decreased with increasing temperature up to 95 °C on account of the decrease in the particle volume fraction in the colloidal glass. However, the moduli increased again due to the formation of the interconnected network of the aggregated PBnMA-*g*-NPs at higher temperatures.

Notably, the colloidal glass, consisting of relatively monodispersed polymer-grafted NPs, shows angle-independent structural colors from blue to green and red with a decrease in the concentration of the particles (Fig. 7a, b) [45]. The theoretical works suggest that the angle-independent and non-brilliant structural color is due to the coherent scattering of visible light from the isotropic nanostructures with short-range order [46]. The TEM image and corresponding ring-shaped two-dimensional (2D) Fourier power spectra confirmed that the short-range ordered glassy structure led to the angle-independent structural colors (Fig. 7c, d). The slightly opaque color was due to the combination of incoherent scattering from the amorphous structure in the long-range and coherent scattering from the ordered structure in the short-range.

Furthermore, the maximum wavelength of the reflection spectra (λ_{max}) can be empirically described as $\lambda_{max} \approx 2\, n_{ave} d$, where d is the mean particle distance and n_{ave} is the average refractive index for the colloidal glass [37]. These results encourage us to tune the angle-independent structural color with temperature. For the colloidal glass of PBnMA-*g*-NPs, the structural color disappeared above the T_c, and the sample became an opaque gel [44]. As seen in Fig. 8a, the peak intensity of the reflection spectrum decreased with increasing temperature, and no peak was observed at 89 °C. This is associated with the above-mentioned "colloidal glass to gel transition"; the short-range ordered structure in the glass state was transformed into a completely disordered structure in the gel state. Therefore, the random light scattering of the aggregated PBnMA-*g*-NPs dominated the gel state. In a subsequent attempt, the colloidal glass was prepared with di-block copolymer-grafted NPs, (PBnMA-*b*-PMMA)-*g*-NPs in order to mitigate the

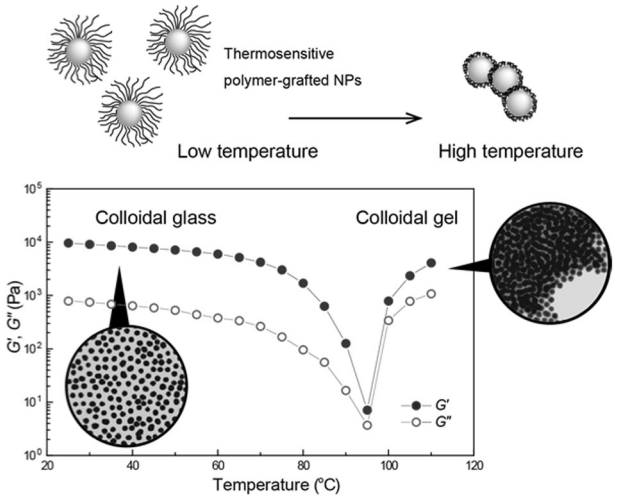

Fig. 6 Schematic illustration for thermosensitive polymer-grafted NPs. Temperature dependence of the elastic modulus (closed circles) and viscous modulus (open circles) of the colloidal glass with 25.0 wt% PBnMA-*g*-NPs ($M_n = 101$ kDa) in [C_2mim][NTf_2] and the pertinent TEM images

colloidal aggregation at temperatures above the T_c of PBnMA groups [47]. In this case, the reflection spectrum shifted to a shorter wavelength at a higher temperature, but no significant decrease in peak intensity was observed (Fig. 8b). The short-range ordered structure could be retained even above the T_c, but the mean particle distance (d) of the colloidal glass decreased because of the desolvation of the PBnMA moieties. The peak shift in this attempt was not large enough to tune the structural color; therefore, factors such as the size of the NPs and the molecular weight of the grafted polymers need to be optimized to tune the angle-independent structural color over the whole color range.

Conclusion

Different fundamental studies on the colloidal stability of silica NPs in ILs are highlighted with a focus on three different repulsive interactions: electrostatic, solvation, and steric forces. A significant charge screening effect in the ILs makes the electrostatic force insufficient for separating the

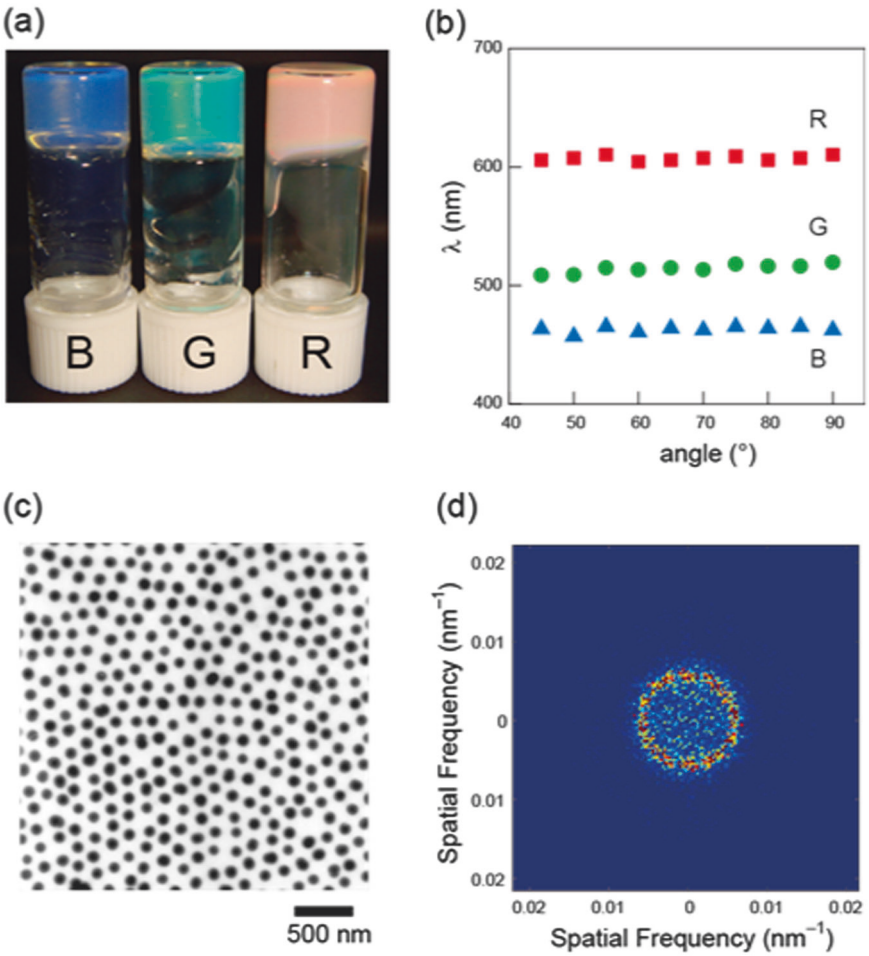

Fig. 7 **a** Photograph of the colloidal glass of PMMA-*g*-NPs ($M_n = 91$ kDa) in [C_2mim][NTf_2]: (B) 33.3 wt%, (G) 25.0 wt%, and (R) 14.2 wt%. **b** Characteristic wavelength (λ) measured as a function of the angle between the incident light and the supported glass substrate. **c** TEM image. **d** corresponding 2D Fourier power spectrum of the colloidal glass G

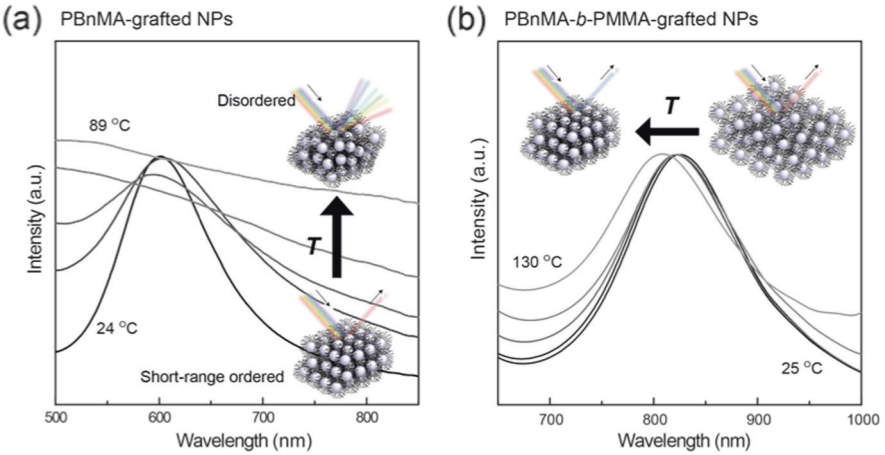

Fig. 8 Temperature dependence of the reflection spectra of the colloidal glass with (**a**) 25 wt% PBnMA-*g*-NPs ($M_n = 101$ kDa) and (**b**) 15 wt% (PBnMA-b-PMMA)-*g*-NPs ($M_n = 103$ kDa) in [C_2mim][NTf_2]

NPs. Alternatively, the solvation and steric forces can act as valid repulsive forces to stabilize the NPs in the ILs. An IL-based solvation force was proposed to account for the experimental evidence of unusual colloidal stabilization in the ILs in absence of any stabilizer. These stabilizer-free colloidal stabilizations should be more pronounced in ILs where the amphiphilicity of ILs can promote the encapsulation of colloidal particles. The intrinsic structure-forming properties of ILs can also contribute to the formation of a well-defined layered structure on a colloidal surface (i.e., IL-based solvation forces).

Two different soft materials were formed by the self-assembly of colloidal NPs in ILs based on colloidal stability. Colloidal gels were prepared using unstable silica NPs that formed an aggregated network in the IL, while colloidal glasses were formed by highly concentrated suspensions of sterically stabilized polymer-grafted NPs. For preparing IL-based solid electrolytes, the present colloidal approach may become a reasonable pathway to ensure liquid-like high ionic conductivity and solid-like high mechanical strength. Shear-induced fluidic properties may be an advantage in terms of facile processability. A variety of different rheological responses of the colloidal systems of ILs may also be promising for their use in functional rheological fluids. Although silica NPs and PMMA/PBnMA were used as model core-particles and grafted polymers, respectively, many other functional colloidal particles and polymers are expected to be applicable in IL-based colloidal gels and glasses.

Acknowledgment

The author is deeply grateful to Prof. Masayoshi Watanabe, Dr. Takeshi Ueki, Prof. Kazue Kurihara, Prof. Masashi Mizukami, Dr. Motohiro Kasuya, and all colleagues for their collaborative works and fruitful discussions. This work was supported in part by a JSPS Grant-in-Aid for JSPS Fellows Grant Number 08J02437.

Compliance with ethical standards

Conflict of interest The authors declare that they have no conflict of interest.

References

1. Marr PC, Marr AC. Ionic liquid gel materials: applications in green and sustainable chemistry. Green Chem. 2016;18:105–28.
2. Carlin RT, Fuller J. Ionic liquid-polymer gel catalytic membrane. Chem Commun. 1997. p.1345–6.
3. MacFarlane DR, Forsyth M, Howlett PC, Kar M, Passerini S, Pringle JM, et al. Ionic liquids and their solid-state analogues as materials for energy generation and storage. Nat Rev Mater. 2016;1:15005.
4. Watanabe M, Thomas ML, Zhang S, Ueno K, Yasuda T, Dokko K. Application of ionic liquids to energy storage and conversion materials and devices. Chem Rev. 2017;117:7190–239.
5. Cowan MG, Gin DL, Noble RD. Poly(ionic liquid)/ionic liquid ion-gels with high "free" ionic liquid content: platform membrane materials for CO_2/light gas separations. Acc Chem Res. 2016;49:724–32.
6. Gu Y, Cussler EL, Lodge TP. ABA-triblock copolymer ion gels for CO_2 separation applications. J Membr Sci. 2012;423-424:20–26.
7. Ranjbaran F, Kamio E, Matsuyama H. Ion gel membrane with tunable inorganic/organic composite network for CO_2 separation. Ind Eng Chem Res. 2017;56:12763–72.
8. Susan MABH, Kaneko T, Noda A, Watanabe M. Ion gels prepared by in situ radical polymerization of vinyl monomers in an ionic liquid and their characterization as polymer electrolytes. J Am Chem Soc. 2005;127:4976–83.
9. He Y, Boswell PG, Bühlmann P, Lodge TP. Ion gels by self-assembly of a triblock copolymer in an ionic liquid. J Phys Chem B. 2007;111:4645–52.
10. Yeon S-H, Kim K-S, Choi S, Cha J-H, Lee H. Characterization of PVdF(HFP) gel electrolytes based on 1-(2-hydroxyethyl)-3-methyl imidazolium ionic liquids. J Phys Chem B. 2005;109:17928–35.
11. Yasuda T, Nakamura S, Honda Y, Kinugawa K, Lee S-Y, Watanabe M. Effects of polymer structure on properties of sulfonated polyimide/protic ionic liquid composite membranes for nonhumidified fuel cell applications. ACS Appl Mater Interfaces. 2012;4:1783–90.
12. Ohno H, Yoshizawa M, Ogihara W. A new type of polymer gel electrolyte: zwitterionic liquid/polar polymer mixture. Electrochim Acta. 2003;48:2079–83.

13. Le Bideau J, Viau L, Vioux A. Ionogels, ionic liquid based hybrid materials. Chem Soc Rev. 2011;40:907–25.
14. Wang P, Zakeeruddin SM, Comte P, Exnar I, Grätzel M. Gelation of ionic liquid-based electrolytes with silica nanoparticles for quasi-solid-state dye-sensitized solar cells. J Am Chem Soc. 2003;125:1166–7.
15. Liu AJ, Nagel SR. Jamming is not just cool any more. Nature. 1998;396:21–22.
16. Stokes JR, Frith WJ. Rheology of gelling and yielding soft matter systems. Soft Matter. 2008;4:1133–40.
17. Pusey PN, van Megen W. Phase behaviour of concentrated suspensions of nearly hard colloidal spheres. Nature. 1986;320:340.
18. Endres F. Ionic liquids: solvents for the electrodeposition of metals and semiconductors. Chemphyschem. 2002;3:144–54.
19. Dupont J, Fonseca GS, Umpierre AP, Fichtner PFP, Teixeira SR. Transition-metal nanoparticles in imidazolium ionic liquids: recycable catalysts for biphasic hydrogenation reactions. J Am Chem Soc. 2002;124:4228–9.
20. Fukushima T, Kosaka A, Ishimura Y, Yamamoto T, Takigawa T, Ishii N, et al. Molecular ordering of organic molten salts triggered by single-walled carbon nanotubes. Molecular ordering of organic molten salts triggered by single-walled carbon nanotubes. Science. 2003;300:2072–4.
21. Torimoto T, Tsuda T, Okazaki K, Kuwabata S. New frontiers in materials science opened by ionic liquids. Adv Mater. 2010;22:1196–221.
22. Israelachvili JN. Intermolecular and surface forces. 3rd ed. Burlington, MA, USA: Academic Press; 2011. p. 253–89.
23. Israelachvili JN. Intermolecular and surface forces. 3rd ed. Burlington, MA, USA: Academic Press; 2011. p. 291–340.
24. Ueno K, Inaba A, Kondoh M, Watanabe M. Colloidal stability of bare and polymer-grafted silica nanoparticles in ionic liquids. Langmuir. 2008;24:5253–9.
25. Lin MY, Lindsay HM, Weitz DA, Ball RC, Klein R, Meakin P. Universality in colloid aggregation. Nature. 1989;339:360–2.
26. Ueno K, Hata K, Katakabe T, Kondoh M, Watanabe M. Nanocomposite ion gels based on silica nanoparticles and an ionic liquid: ionic transport, viscoelastic properties, and microstructure. J Phys Chem B. 2008;112:9013–9.
27. Khan SA, Zoeller NJ. Dynamic rheological behavior of flocculated fumed silica suspensions. J Rheol. 1993;37:1225–35.
28. Ueno K, Imaizumi S, Hata K, Watanabe M. Colloidal interaction in ionic liquids: effects of ionic structures and surface chemistry on rheology of silica colloidal dispersions. Langmuir. 2009;25:825–31.
29. Ueno K, Kasuya M, Watanabe M, Mizukami M, Kurihara K. Resonance shear measurement of nanoconfined ionic liquids. Phys Chem Chem Phys. 2010;12:4066–71.
30. Israelachvili JN. Intermolecular and surface forces. 3rd ed. Burlington, MA, USA: Academic Press; 2011. p. 341–80.
31. Hayes R, Warr GG, Atkin R. Structure and nanostructure in ionic liquids. Chem Rev. 2015;115:6357–426.
32. Hayes R, Warr GG, Atkin R. At the interface: solvation and designing ionic liquids. Phys Chem Chem Phys. 2010;12:1709–23.
33. Smith JA, Werzer O, Webber GB, Warr GG, Atkin R. Surprising particle stability and rapid sedimentation rates in an ionic liquid. J Phys Chem Lett. 2010;1:64–68.
34. Gao J, Ndong RS, Shiflett MB, Wagner NJ. Creating nanoparticle stability in ionic liquid $[C_4mim][BF_4]$ by inducing solvation layering. ACS Nano. 2015;9:3243–53.
35. Zhang H, Dasbiswas K, Ludwig NB, Han G, Lee B, Vaikuntanathan S, Talapin DV. Stable colloids in molten inorganic salts. Nature. 2017;542:328.
36. Israelachvili JN. Intermolecular and surface forces. 3rd ed. Burlington, MA, USA: Academic Press; 2011. p. 133–49.
37. Ueno K, Sano Y, Inaba A, Kondoh M, Watanabe M. Soft glassy colloidal arrays in an ionic liquid: colloidal glass transition, ionic transport, and structural color in relation to microstructure. J Phys Chem B. 2010;114:13095–103.
38. Ueno K, Fukai T, Nagatsuka T, Yasuda T, Watanabe M. Solubility of poly(methyl methacrylate) in ionic liquids in relation to solvent parameters. Langmuir. 2014;30:3228–35.
39. Batista MLS, Neves CMSS, Carvalho PJ, Gani R, Coutinho JAP. Chameleonic behavior of ionic liquids and its impact on the estimation of solubility parameters. J Phys Chem B. 2011;115:12879–88.
40. Huang Y, Takata A, Tsujii Y, Ohno K. Semisoft colloidal crystals in ionic liquids. Langmuir. 2017;33:7130–6.
41. Unemoto A, Matsuo T, Ogawa H, Gambe Y, Honma I. Development of all-solid-state lithium battery using quasi-solidified tetraglyme-lithium bis(trifluoromethanesulfonyl)amide–fumed silica nano-composites as electrolytes. J Power Sources. 2013;244:354–62.
42. Chen N, Zhang H, Li L, Chen R, Guo S. Ionogel electrolytes for high-performance lithium batteries: a review. Adv Energy Mater. 2018;8:1702675.
43. Ueki T. Stimuli-responsive polymers in ionic liquids. Polym J. 2014;46:646–55.
44. Ueno K, Inaba A, Ueki T, Kondoh M, Watanabe M. Thermosensitive, soft glassy and structural colored colloidal array in ionic liquid: colloidal glass to gel transition. Langmuir. 2010;26:18031–8.
45. Ueno K, Inaba A, Sano Y, Kondoh M, Watanabe M. A soft glassy colloidal array in ionic liquid, which exhibits homogeneous, non-brilliant and angle-independent structural colours. Chem Commun. 2009. p.3603–5.
46. Jin C, Meng X, Cheng B, Li Z, Zhang D. Photonic gap in amorphous photonic materials. Phys Rev B. 2001;63:195107.
47. Ueno K, Fukai T, Watanabe M. Thermosensitive soft glassy colloidal arrays of block-copolymer-grafted silica nanoparticles in an ionic liquid. Polym J. 2015;48:289–94.

Kazuhide Ueno is an associate professor at Yokohama National University. He received his Ph.D. degree in 2009 from Yokohama National University. He was a postdoctoral fellow at Tohoku University with Prof. Kazue Kurihara (2010), at Arizona State University with Prof. C. Austen Angell (2010–2012), and at Yokohama National University with Prof. Masayoshi Watanabe (2012–2014). He joined Yamaguchi University as an assistant professor in 2015, and moved to Yokohama National University in 2017. His research interests include ionic liquid based soft materials and battery electrolytes.